ACS APPLIED MATERIALS & INTERFACES
RESEARCH ARTICLE
www.acsami.org

Enhanced Free Exciton and Direct Band-Edge Emissions at Room Temperature in Ultrathin ZnO Films Grown on Si Nanopillars by Atomic Layer Deposition

Yuan-Ming Chang,[*,†] Jiann Shieh,[‡] Pei-Yuan Chu,[†] Hsin-Yi Lee,[§,⊥] Chih-Ming Lin,[#] and Jenh-Yih Juang[*,†]

[†]Department of Electrophysics and [⊥]Department of Materials Science and Engineering, National Chiao Tung University, Hsinchu 300, Taiwan

[‡]Department of Materials Science and Engineering, National United University, Miaoli 360, Taiwan

[§]National Synchrotron Radiation Research Center, Hsinchu 300, Taiwan

[#]Department of Applied Science, National Hsinchu University of Education, Hsinchu 300, Taiwan

ABSTRACT: Room-temperature ultraviolet (UV) luminescence was investigated for the atomic layer deposited ZnO films grown on silicon nanopillars (Si-NPs) fabricated by self-masking dry etching in hydrogen-containing plasma. For films deposited at 200 °C, an intensive UV emission corresponding to free-exciton recombination (∼3.31 eV) was observed with a nearly complete suppression of the defect-associated broad visible range emission peak. On the other hand, for ZnO films grown at 25 °C, albeit the appearance of the defect-associated visible emission, the UV emission peak was observed to shift by ∼60 meV to near the direct band edge (3.37 eV) recombination emission. The high-resolution transmission electron microscopy (HRTEM) showed that the ZnO films obtained at 25 °C were consisting of ZnO nanocrystals with a mean radius of 2 nm embedded in a largely amorphous matrix. Because the Bohr radius of free-exictons in bulk ZnO is ∼2.3 nm, the size confinement effect may have occurred and resulted in the observed direct band edge electron−hole recombination. Additionally, the results also demonstrate order of magnitude enhancement in emission efficiency for the ZnO/Si-NP structure, as compared to that of ZnO directly deposited on Si substrate under the same conditions.

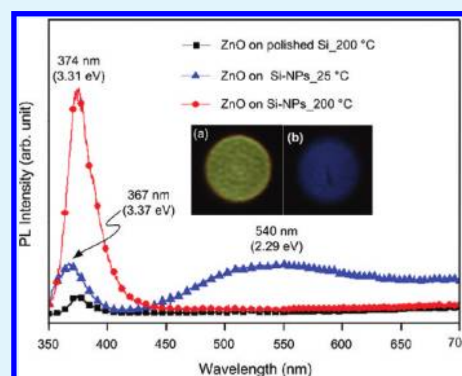

KEYWORDS: ultrathin, ZnO, Si nanopillars, atomic layer deposition, free exciton

INTRODUCTION

Recently, ZnO has become one of the most prominent materials for optoelectronic applications, namely for ultraviolet photodetectors,[1] optical waveguides,[2] and field-effect transistors.[3,4] In particular, the wide band gap of 3.37 eV and the large exciton binding energy of 60 meV (much higher than that of ZnSe (40 meV) and GaN (25 meV)[5]) inherent to ZnO have been demonstrated to exhibit efficient excitonic emission at room temperature. Consequently, considerable efforts have been devoted to this particular material in order to harvest efficient ultraviolet luminescence (UVL) from ZnO.[6−8] However, to obtain enough emission intensity previous approaches usually required relatively thick ZnO films with a thickness of 100 nm or more and sometimes have to resort to more time-consuming fabrication processes. For instance, pulsed laser deposition (PLD) and RF magnetron sputtering have been the most common approaches used to fabricate ZnO thin films for optoelectronic devices. These two methods, however, either requires a high growth temperature of 350 °C (PLD) or post-growth annealing for obtaining desired properties. On the other hand, atomic layer deposition (ALD) is a film growth technique characterized by unique process of self-limiting vapor-phase chemisorption. Thus, depending on consecutive reactions taking place at the substrate surface, the deposited film is essentially growing with a layer-by-layer fashion. The process hence gives rise to excellent step-coverage characteristic as well as good crystalline quality of films even when grown at relatively low substrate temperatures. It has been subsequently proposed that ZnO films grown by using ALD with thickness thinner than 30 nm might serve as a possible viable alternative to resolve the above-mentioned drawbacks for other deposition processes. Unfortunately, because of the relatively small amount of emissive material involved, the emission intensity for the excitonic recombination from the planar thin films obtained by ALD process was often very weak and has seriously hindered the possibility of practical UVL applications. For that matter, it is desirable to develop a viable approach that can harvest UVL from ultrathin ZnO film in a more efficient fashion.

In this study, we demonstrate that by merely raising the substrate temperature to 200 °C during the ALD, not only can the defect-associated visible emission be completely suppressed but also the significantly enhanced UVL emission associated with

Received: August 8, 2011
Accepted: October 3, 2011
Published: October 03, 2011

ACS Publications © 2011 American Chemical Society

free excitonic emission is obtained for ultrathin ZnO film (~10 nm) grown on the Si nanopillar (Si-NP) template. It is believed that the high density ZnO/Si-NP heterostructure (~3 × 10^{12} cm^{-2}) could be the primary factor for obtaining the high surface/volume ratio needed to enhance the light emission. On the other hand, for films grown at room-temperature, evidence of UVL emission from direct band-edge recombinations, presumably because of the effect of size confinement, is observed. Detailed microstructural examinations by high-resolution crosssectional transmission microscopy (HRXTEM) indicate the intimate correlations between the obtained optical properties and film microstructures.

MATERIALS AND METHODS

The wafer-scale production of Si-NPs was carried out in an inductively coupled plasma chemical vapor deposition (ICPCVD) system with the following process. Prior to performing the etching processes, CF_4 and O_2 plasma were applied to clean the chamber. After the Si(100) wafer was loaded into the reaction chamber, it was pumped to a pressure of 5 × 10^{-5} Torr with the substrate holder being heated to 400 °C. Subsequently, the H_2 gas with a flow rate of 160 sccm was introduced into the reactor with the pressure being kept at 30 mTorr. The etching process was carried out by applying a radio frequency (RF) power of 550 W with a dc-bias power being maintained at 280 W. Details of the processes and the possible mechanisms involved in obtaining Si-NPs with the H_2-plasma etching were described and discussed previously.[9−11]

ZnO films with thickness in few tens of nanometers were prepared by an ALD system and grown on either polished Si (p-type, (100) orientation) or Si-NPs under the ambient temperature (~25 °C) or 200 °C. In particular, critical purge steps were carried out to prevent the reactive precursors from interacting with each other.[12] Briefly, the pulse durations of water vapor and diethylzinc (DEZn) were kept at 100 and 50 ms, respectively. The stock time for both water vapor and DEZn was set to 15 s in the stock mode. The purge and pumping periods were both fixed at 15 s and N_2 was used as the purge gas with the pressure being set to 5 × 10^{-2} Torr. The ultrathin ZnO films were prepared with 30 ALD cycles, which gives a film thickness of about 10 nm.

The crystallographic structure of the ZnO/Si-NP samples was characterized by the grazing incidence XRD at the wiggler beamline BL-17B1 in the National Synchrotron Radiation Research Center (NSRRC), Hsinchu, Taiwan. The incident X-ray was focused vertically with a mirror and made monochromatic with energy 8 keV by a Si (111) double-crystal monochromator. The morphology of the obtained ZnO/Si-NPs was examined using a FESEM (JEOL JSM-6700F). The compositions of the obtained thin films were analyzed using the energy-dispersive X-ray spectroscopy (EDS) attached to the FESEM. Cross-sectional lattice images of the ultrathin ZnO/Si-NPs were obtained by using a transmission electron microscope (TEM, JEOL JEM-2010F) operated at a voltage of 200 kV. The measurements of photoluminescence (PL) were performed at room temperature using He−Cd laser (325 nm, IK3252R-E, Kimmon) for excitation and a CCD (80 K, Spec-10, Princeton Instruments) with a monochromator (0.5 m, SP-2558A, Acton) for detection.

RESULTS AND DISCUSSION

Figure 1a shows the typical cross-sectional image of the ZnO/Si-NPs viewed by the field emission scanning electron microscope (FESEM). It appears that the morphology of the vertically aligned Si-NPs remains essentially intact after depositing the ZnO films by ALD processes. Although a thin layer with relatively brighter contrast is suggestive of the existence of the deposited ZnO film,

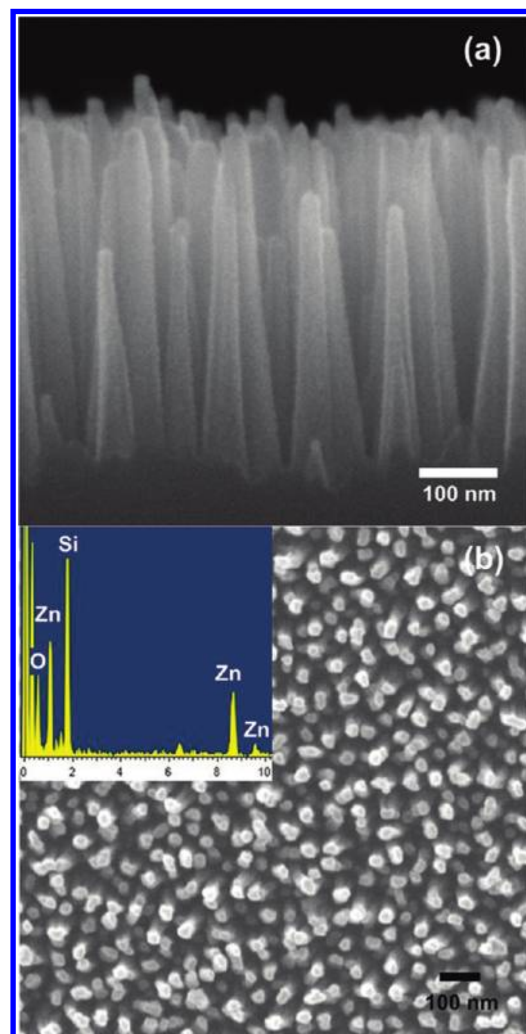

Figure 1. (a) Cross-sectional and (b) top-view SEM images of ultrathin ZnO film which grown at 200 °C on ZnO/Si-NPs. The inset in b is the EDS analysis.

further evidence are certainly needed to verify the conjectures. Thus, we show in the inset of Figure 1b the EDS spectrum for the 10 nm-thick ZnO/Si-NPs films obtained at 200 °C by ALD. The spectrum evidently indicates the existence of thin ZnO layers on Si-NPs. In addition, as shown in Figure 1b, the top-view SEM image reveals a facet-like appearance at the tip of the Si-NP template. This suggests that either the Si-NPs or the deposited ZnO films are in crystalline state, albeit the nominal thickness of the ZnO films was only about 10 nm. The X-ray diffraction (XRD) and TEM results to be displayed below also give rise to similar conclusions. The density of the ZnO/Si-NPs heterostructure is estimated to be around 3 × 10^{12} cm^{-2} with an average height of ~600−700 nm, giving rise to a high surface/volume ratio needed for enhancing the light emission.

To further delineate the effect of growth temperature on the crystalline structure of the ultrathin ZnO films obtained by the current ALD process, we performed grazing incidence XRD measurements. Figure 2 shows the XRD traces obtained for the 10 nm thick ZnO films deposited on Si-NPs at growth temperature of 25 or 200 °C, respectively. It is evident that, for ZnO film grown at 200 °C, there are three distinctive diffraction peaks corresponding to (100), (002), and (101) crystallographic orientations of the hexagonal ZnO, while only barely discernible (101) diffraction peak is observed for that deposited

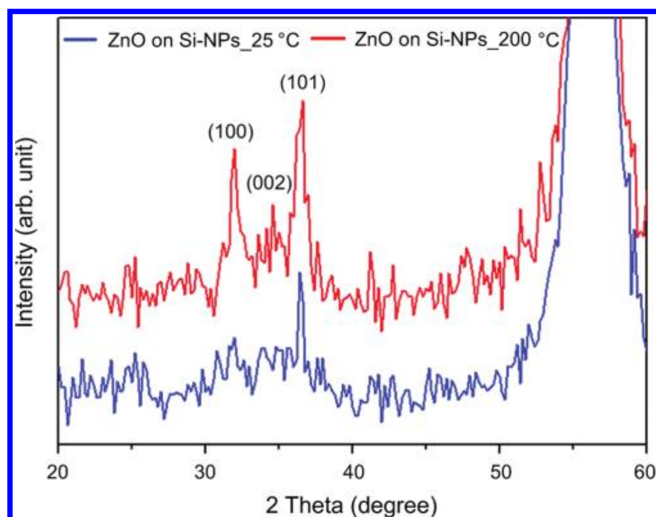

Figure 2. XRD spectra of ultrathin ZnO films respectively grown at 25 and 200 °C on Si-NPs templates.

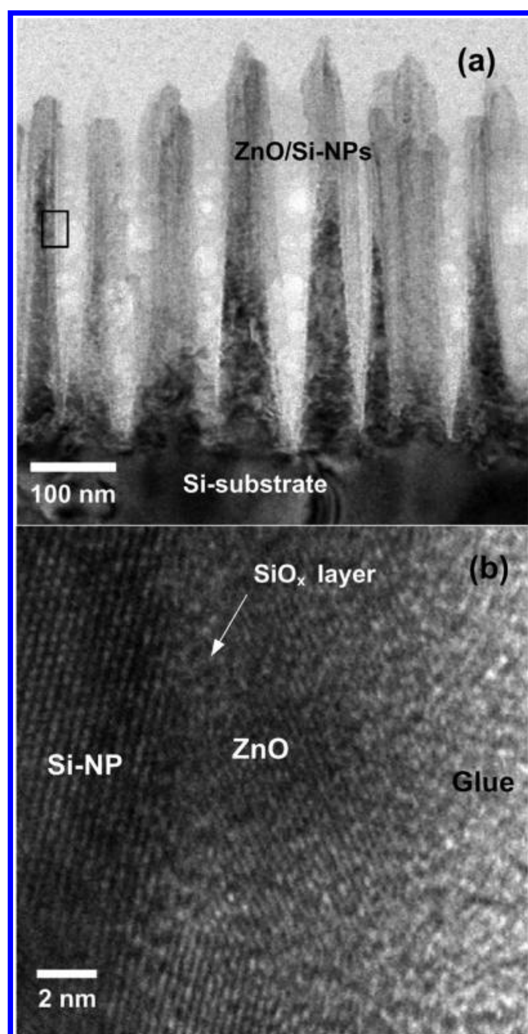

Figure 3. Images of (a) TEM and (b) HRTEM for the ZnO/Si-NP heterostructure gown at 200 °C.

at 25 °C. The results suggest that the ultrathin ZnO film deposited on the Si-NPs at 200 °C, while remains largely polycrystalline, is of good crystalline quality. On the other hand, the microstructure of the ZnO film obtained at 25 °C might be consisting of only nanosized grains dispersed in a largely amorphous matrix.[13]

To further verify the conjectures derived from the XRD results described above, we examined the ZnO/Si-NPs heterostructures deposited at 200 °C by carrying out the high-resolution transmission electron microscopy (HRTEM). Figure 3a displays the cross-sectional TEM image of the Si-NPs coated with a layer of 10 nm-thick ZnO film. In addition to display the similar pillar-like morphology shown in Figure 1a, the image further reveals that the average interpillar spacing is about 50 nm and there appears a thin layer covering continuously over the entire pillar (see, for example, the pillar marked with a rectangle in Figure 3(a). The layer, as will be examined further below, indeed is ZnO film and thus demonstrates the unique power of ALD process in obtaining excellent step coverage for structures with high aspect ratios. Figure 3b shows the HRTEM image for the area marked by the small rectangle, revealing the close-up look at the interface of ZnO/Si-NPs heterostructures. It clearly displays the nearly intact single-crystalline characteristics of the Si-NPs obtained by the reduced H_2 plasma etching process and a layer of continuous polycrystalline ZnO film, separated occasionally by regions of amorphous SiO_x. It is noted that, despite of the existence of the amorphous SiO_x regions at the interface, the ZnO layer is of very good crystalline quality over the entire thickness of 10 nm, which is consistent with the conjectures derived from the XRD results. The next question to be addressed is how the detailed film microstructure affects the optical properties of ultrathin ZnO films grown on Si-NPs.

Because of the many attractive optical properties ubiquitously exhibited in ZnO films and various ZnO nanostructures, the PL properties of ZnO have been the subject of extensive research.[14−17] In this respect, we compare the room-temperature PL spectra of the ultrathin ZnO films deposited at growth temperatures of 25 and 200 °C, as shown in Figure 4. For comparison, the PL spectrum of the ZnO film grown on polished Si at 200 °C is also included in Figure 4. It is immediately noticed that there are distinctive features between the PL spectra obtained for films grown at 25 °C and that grown at 200 °C. First, the spectrum for the ultrathin ZnO films deposited on Si-NPs at 25 °C (solid triangles) shows both an emission peak centering at 367 nm (3.37 eV) and a broadened spectrum covering almost the entire visible range with the peak locating around 540 nm. The strong intensity of the latter indeed exhibits the greenish emission displayed in inset picture a taken by the digital camera. The visible emissions are generally conceived to originate primarily from the defect-related in ZnO, such as oxygen or zinc-related defects.[18−23] More specifically, the visible emission has been attributed to donor−acceptor pair transitions involving oxygen vacancies.[24,25] In any case, the fact that the comparable PL intensities of the band-edge exciton recombination and the defect-related visible emission indicates that, due to the low growth temperature, the ZnO films grown on Si-NPs at 25 °C may have inherited significant amount of atomic scale defects. The results for films grown at 200 °C, on the other hand, display a nearly complete suppression of visible range emission. This lends strong evidence to that the films are indeed with good crystalline quality and the UV emission (3.31 eV peak) is primarily resulting from the free excitons.[26−29] The high crystallinity of the ZnO films obtained at higher growth temperature apparently have eliminated most of the structural defects which not only blocked the self-compensation processes thermodynamically but also removed most of the non-radiative recombination channels. Moreover, it is important to note

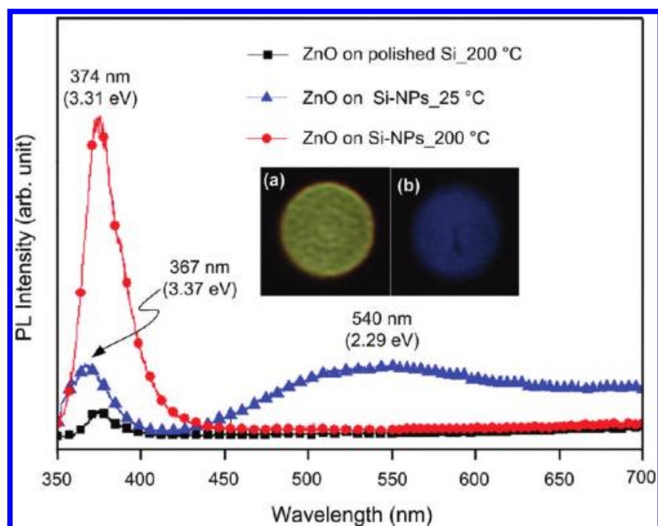

Figure 4. Room-temperature PL spectra obtained for the ZnO thin films grown on polished Si, and ZnO/Si-NP heterostructures at growth temperatures of 25 and 200 °C. The insets (a) and (b) show the bright green or blue-violet emission taken from 10 nm thick ZnO/Si-NP heterostructures (grown at 25 or 200 °C).

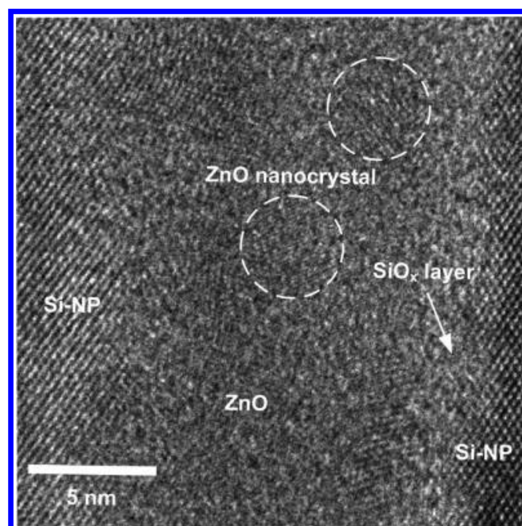

Figure 5. HRTEM image of ZnO/Si-NPs grown at 25 °C.

that the intensity of the free exciton emission at 374 nm (3.31 eV) for the ZnO/Si-NPs structure (solid circles in Figure 4) was enhanced by nearly an order of magnitude as compared to that obtained from ZnO/Si (solid squares in Figure 4), albeit both were deposited under exactly the same conditions. This is attributed to the high aspect (surface/volume) ratio inherent to the Si-NPs, which has allowed considerably more amount of ZnO material to be grown on the template and led to markedly more efficient UV emission.[13] The fact that the two 10 nm thick ZnO films deposited on polished Si and Si-NPs under exactly the same conditions displays essentially the same PL emission characteristics, except for the relative intensities, further indicates the unique feature of the current ALD processes, in that the film crystalline structure appears to depend intimately on the growth temperature regardless of the detailed conditions of the substrate used. In any case, the current results have demonstrated a viable way of obtaining efficient intrinsic UV emission from ZnO films. Inset b of Figure 4 displays the digital camera picture of the blue-violet emission from the ZnO films grown on Si-NPs at 200 °C. It is interesting to note that the two digital camera pictures are visibly reflecting what one would expect to see on the basis of the results of the PL measurements.

Finally, we turn to discuss the origin of the UV-emission peak centering at 367 nm (3.37 eV), which coincidentally has the same energy as the energy gap of bulk ZnO. Thus, it is suggestive that the emission may have originated from direct band edge electron−hole recombination, which in general is not expected to occur for ionic semiconductors with large exciton binding energy, such as in the case of ZnO. In fact, to the best of our knowledge, this could be the first observation of room-temperature band-to-band emission (3.37 eV) for ZnO. Although there have been extensive investigations concerning the effects of quantum confinement on the UV emissions in various ZnO nanostructures,[8,30−33] the observed emissions were either associated with the free excitons,[8,24] acceptor-bound excitons,[31] or with excited excitonic states.[32,33] Thus, the relevant energies were all significantly deviated from the bandgap energy of 3.37 eV. On the other hand, it has been pointed out that in ionic materials, the exciton−optical phonon interaction can significantly influence their optical properties.[34] In particular, the polaronic corrections favors more bound excitons with smaller sizes. For ZnO, in addition to a 60 meV exciton binding energy mentioned above, the Bohr radius of the free excitons is ∼2.34 nm.[34] It is thus quite possible that the 3.37 eV UV emission observed in the ultrathin ZnO films grown on Si-NPs at 25 °C is a consequence of size confinement. Namely, it is due to recombination of electron−hole pairs, which were unable to form excitons because the crystal size is compatible or even smaller than the Bohr radius. Indeed, as displayed in Figure 5, the film miscrostructure of the ZnO/Si-NPs obtained at 25 °C evidently exhibit a distinct feature of ZnO nanocrystals dispersing in a largely amorphous matrix. As indicated by the dashed circle shown in Figure 5, the average radius of the ZnO nanocrystals embedded in the amorphous matrix is ∼2 nm, which is slightly smaller than the Bohr radius of the free excitons (∼2.3 nm). This lends supportive evidence of attributing the 3.37 eV emission to the direct band-to-band transition of electrons and holes residing at respective band edges of ZnO.[35]

CONCLUSION

In summary, we have successfully demonstrated the feasibility of utilizing a novel ZnO/Si-NP heterostructure to obtain highly efficient room-temperature UV emission. For the ZnO/Si-NP heterostructures obtained at 200 °C, the structural and optical properties analyses evidently indicate that the observed UV emissions are intimately related to the highly crystalline ZnO layers resulted from high temperature ALD processes. More importantly, by growing ZnO films on the Si-NPs evidently gives rise to an enhancement of the UV emission intensity by nearly an order of magnitude as compared to its ZnO/polished-Si counterpart, presumably due to the significantly increased surface area needed. For the ZnO/Si-NP heterostructures obtained at 25 °C, in addition to the defect-associated visible emission, the UV-emission in this case, instead of resulting from the free exciton recombination, appears to result from direct band-to-band electron−hole recombination. The relevant microstructural analyses suggest that the effect of size confinement might have been the primary reason for the observed behaviors.

AUTHOR INFORMATION

Corresponding Author
*Phone: +886-3-5712121, ext. 56116. Fax: +886-3-5725230. E-mail: ymchang7@gmail.com (Y.-M.C.); jyjuang@g2.nctu.edu.tw (J.-Y.J.).

ACKNOWLEDGMENT

This work was partially supported by the National Science Council of Taiwan, under Grant NSC 100-2811-M-009-037. J.-Y.J. is supported in part by the National Science Council of Taiwan and the MOE-ATP program operated at NCTU. The authors also thank Dr. Yu-Hwa Shih, Dr. Jheng-Ming Huang (NCTU), Dr. Shang-Jui Chiu (NTHU), Dr. Yen-Ting Liu (NCTU), Yan-Chen Chen, and Chih-Ming Wu (NDL) for useful discussions; Yi-Ling Jian for SEM; and Dr. Chien-Ting Wu for TEM techniques supported in National Nano Device Laboratories (NDL).

REFERENCES

(1) Peng, S.-M.; Su, Y.-K.; Ji, L.-W.; Wu, C.-Z.; Cheng, W.-B.; Chao, W.-C. *J. Phys. Chem. C* **2010**, *114*, 3204–3208.
(2) Law, M.; Sirbuly, D. J.; Johnson, J. C.; Goldberger, J.; Saykally, R. J.; Yang, P. D. *Science* **2004**, *305*, 1269–1273.
(3) Suh, D.-I.; Lee, S.-Y.; Hyung, J.-H.; Kim, T.-H.; Lee, S.-K. *J. Phys. Chem. C* **2008**, *112*, 1276–1281.
(4) Wang, X.; Zhou, J.; Song, J.; Liu, J.; Xu, N.; Wang, Z. L. *Nano Lett.* **2006**, *6*, 2768–2772.
(5) Rodina, A. V.; Dietrich, M.; Göldner, A.; Eckey, L.; Hoffmann, A.; Efros, A. L.; Rosen, M.; Meyer, B. K. *Phys. Rev. B* **2001**, *64*, 115204–1−19.
(6) Huang, M. H.; Mao, S.; Feick, H.; Yan, H.; Wu, Y.; Kind, H.; Weber, E.; Russo, R.; Yang, P. *Science* **2001**, *292*, 1897–1899.
(7) Liu, C.; Zapien, J. A.; Yao, Y.; Meng, X.; Lee, C. S.; Fan, S.; Lifshitz, Y.; Lee, S. T. *Adv. Mater.* **2003**, *15*, 838–841.
(8) Kong, Y. C.; Yu, D. P.; Zhang, B.; Fang, W.; Feng, S. Q. *Appl. Phys. Lett.* **2001**, *78*, 407–409.
(9) Shieh, J.; Lin, C. H.; Yang, M. C. *J. Phys. D: Appl. Phys.* **2007**, *40*, 2242–2246.
(10) Yang, M. C.; Shieh, J.; Hsu, C. C.; Cheng, T. C. *Electrochem. Solid-State Lett.* **2005**, *8*, C131–C133.
(11) Shieh, J.; Hou, F. J.; Chen, Y. C.; Chen, H. M.; Yang, S. P.; Cheng, C. C.; Chen, H. L. *Adv. Mater.* **2010**, *22*, 597–601.
(12) Ku, C.-S.; Huang, J.-M.; Lin, C.-M.; Lee, H.-Y. *Thin Solid Films* **2009**, *518*, 1373–1376.
(13) Chang, Y.-M.; Jian, S.-R.; Lee, H.-Y.; Lin, C.-M.; Juang, J.-Y. *Nanotechnology* **2010**, *21*, 385705–1−7.
(14) Fonoberov, V. A.; Balandin, A. A. *Appl. Phys. Lett.* **2007**, *85*, 5971–5973.
(15) Fonoberov, V. A.; Balandin, A. A. *Phys. Rev. B* **2004**, *70*, 195410–1−5.
(16) Fonoberov, V. A.; Balandin, A. A. *J. Phys: Condens. Matter.* **2005**, *17*, 1085–1097.
(17) Fonoberov, V. A.; Balandin, A. A. *J. Nanoelectron. Optoelectron.* **2006**, *1*, 19–38.
(18) Özgür, Ü.; Alivov, Y. I.; Liu, C.; Teke, A.; Reshchikov, M. A.; Dogan, S.; Avrutin, V.; Cho, S.-J.; Morkoç, H. *J. Appl. Phys.* **2005**, *98*, 041301–1−103.
(19) Kang, H. S.; Kang, J. S.; Kim, J. W.; Lee, S. Y. *J. Appl. Phys.* **2004**, *95*, 1246–1250.
(20) Li, D.; Leung, Y. H.; Djurišic, A. B.; Liu, Z. T.; Xie, M. H.; Shi, S. L.; Xu, S. J.; Chan, W. K. *Appl. Phys. Lett.* **2004**, *85*, 1601–1603.
(21) Gong, Y.; Andelman, T.; Neumark, G. F.; O'Brien, S.; Kuskovsky, I. L. *Nanoscale Res. Lett.* **2007**, *2*, 297–302.
(22) Meng, X. Q.; Shen, D. Z.; Zhang, J. Y.; Zhao, D. X.; Lu, Y. M.; Dong, L.; Zhang, Z. Z.; Liu, Y. C.; Fan, X. W. *Solid State Commun.* **2005**, *135*, 179–182.
(23) Lin, B.; Fu, Z.; Jia, Y. *Appl. Phys. Lett.* **2001**, *79*, 943–945.
(24) Cai, P. F.; You, J. B.; Zhang, X. W.; Dong, J. J.; Yang, X. L.; Yin, Z. G.; Chen, N. F. *J. Appl. Phys.* **2009**, *105*, 083713–1−6.
(25) Djurišic, A. B.; Leung, Y. H. *Small* **2006**, *2*, 944–961.
(26) Wang, L.; Giles, N. C. *J. Appl. Phys.* **2003**, *94*, 973–978.
(27) Lim, J.; Shin, K.; Kim, H. W.; Lee, C. *J. Lumin.* **2004**, *109*, 181–185.
(28) Ogata, K; Sakurai, Sz.; Fujita, Sg.; Matsushige, K. *J. Cryst. Growth* **2000**, *214/215*, 312–315.
(29) Lim, J.; Shin, K.; Kim, H. W.; Lee, C. *Mater. Sci. Eng., B* **2004**, *107*, 301–304.
(30) Xing, Y. J.; Xi, Z. H.; Xue, Z. Q.; Zhang, X. D.; Song, J. H.; Wang, R. M.; Xu, J.; Song, Y.; Zhang, S. L.; Yu, D. P. *Appl. Phys. Lett.* **2003**, *83*, 1689–1691.
(31) Fonoberov, V. A.; Alim, K. A.; Balandin, A. A.; Xiu, F.; Liu, J. *Phys. Rev. B* **2006**, *73*, 165317–1−9.
(32) Gu, Y.; Kuskovsky, I. L.; Yin, M.; O'Brien, S.; Neumark, G. F. *Appl. Phys. Lett.* **2004**, *85*, 3833–3835.
(33) Gu, X. Q.; Zhu, L. P.; Ye, Z. Z.; He, H. P.; Zhang, Y. Z.; Huang, F.; Qiu, M. X.; Zeng, Y. J.; Liu, F.; Jaeger, W. *Appl. Phys. Lett.* **2007**, *91*, 022103–1−3.
(34) Senger, R. T.; Bajaj, K. K. *Phys. Rev. B* **2003**, *68*, 045313–1−8.
(35) Wong, E. M.; Searson, P. C. *Appl. Phys. Lett.* **1999**, *74*, 2939–2941.